時系列情報と空間情報の合成解析による熱環境情報の推定に関する研究

内田, 哲郎 / 大嶋, 太市 / Oshima, Taichi / Uchida, Tetsurou

(出版者 / Publisher)
法政大学工学部
(雑誌名 / Journal or Publication Title)
法政大学工学部研究集報 / 法政大学工学部研究集報
(巻 / Volume)
28
(開始ページ / Start Page)
1
(終了ページ / End Page)
25
(発行年 / Year)
1992-02
(URL)
https://doi.org/10.15002/00003891

時系列情報と空間情報の合成解析による熱環境情報の推定に関する研究

内田哲郎* ・大嶋太市**

A Study of Estimating Thermal Environmental Conditions In Urban Area From Multi-Temporal and Spatial Informations

Tetsurou UCHIDA* and Taichi OSHIMA**

Abstract

Satellite Remote sensing technology using Satellite acquires wide pictures on same area of the earth surface during short period of time. But, the data collected from satellite are affected by atmospheric conditions. The conventional method is necessary the ground truth and air plane data to analyze the temporal thermal data. The thermal characteristics of ground surface is obtained by thermal inertia.

But as a matter of fact, temporal good thermal images are difficult to obtain for being changeable in weather conditions and to get the data only one time a day from satellite. This study airms at investigating the thermal characteristics by temporal and thermal characteristics which have been obtained by texture analysis of thermal images using spatial filter.

Result of texture analysis shows to have been obtained good correlation between thermal characteristics in temporal and spatial.

*M.S. of Engineering (Housei University)

Research Fellow Environmental Engineering, Tokyo Institute of Technology

**Prof. Dr. of Eng.

College of Engineering, Hosei University

1. Introduction

At present, cities are facing with crucial problems such as population centralization and green decreasing.

As the protection voice keeping nature in our society is rising up, remote sensing data are expected to play the key role of sending constantly the significant urban thermal informations being available from wide area and taking advantage of monitoring temporal change for the same areas of earth surface.

However, remote sensing data with multi-temporal informations are not always available for the changeable weather conditions.

Therefore, the thermal environmental monitoring has been performed using the limited data available from remote sensing.

But, it's seldom to obtain the good quality temporal data in normal case. Then, data from airplane and low resolution satellite data are used instead.

LANDSAT,MOS - 1 data are acquired each 16 days for the same area and have the high resolution of 30 to 50m. and it is the most appropriate to catch up the city thermal conditions, but temporal resolving power is low.

Meteorological satellite - NOAA:AVHRR(Advance Very High Resolution Radiometer) has high temporal resolving power and acquire the data 2 times a day, but the spatial resolving power is very low, about 1km.

Therefore it is difficult to extract urban thermal factors for analysis. This study airms at comparing and surveying the thermal data extracted from the multi-temporal images and the thermal images of one definite time and experimentally are discussed the relationship between them.

Result of the texture analysis shows that the good correlations have been obtained from urban thermal environmental informations in temporal and spatial and texture analysis generated noise and the noise elimination was performed using RANG－FILTER and LAPLACIAN－FILTER for the analyzed images and finally discussed on problems of binary transformation.

The result has concluded to be able to estimate the extraction methods for environmental informations by knowing the correlation between temporal and spatial thermal environmental informations under the condition of gaining the texture algorithm.

2. Study Process

This study at first examined the texture algorithm closely related to the urban thermal informations from points of temporal and spatial.

Then, this study investigated relation between areas of the same or different behaviors in both land cover and land use. Fig. 1 illustrates the flow chart of study.

The original images of data have been normalized and calibrated between different band (See A part in Fig. 1).

The multi-temporal and the spatial informations thermal environment from calibrated image (See B part in Fig.1).

But, the noise generated in images of texture and was removed using RANG－FILTER and LAPLACIAN－FILTER (See C part in Fig.1).

Mutual analysis between multi-temporal and spatial informations in thermal environment, was performed by regression analysis (See D part in Fig.1).

Result of texture analysis shows to have been obtained good correlation between multi-temporal and spatial informations of thermal environment.

The most effective parameters for thermal environmental analysis in urban area can be obtained from the quantity of extracted texture and the authors have proposed to be able to observe the thermal environmental factors using remote sensing techniques in temporal and spatial (See E part in Fig. 1).

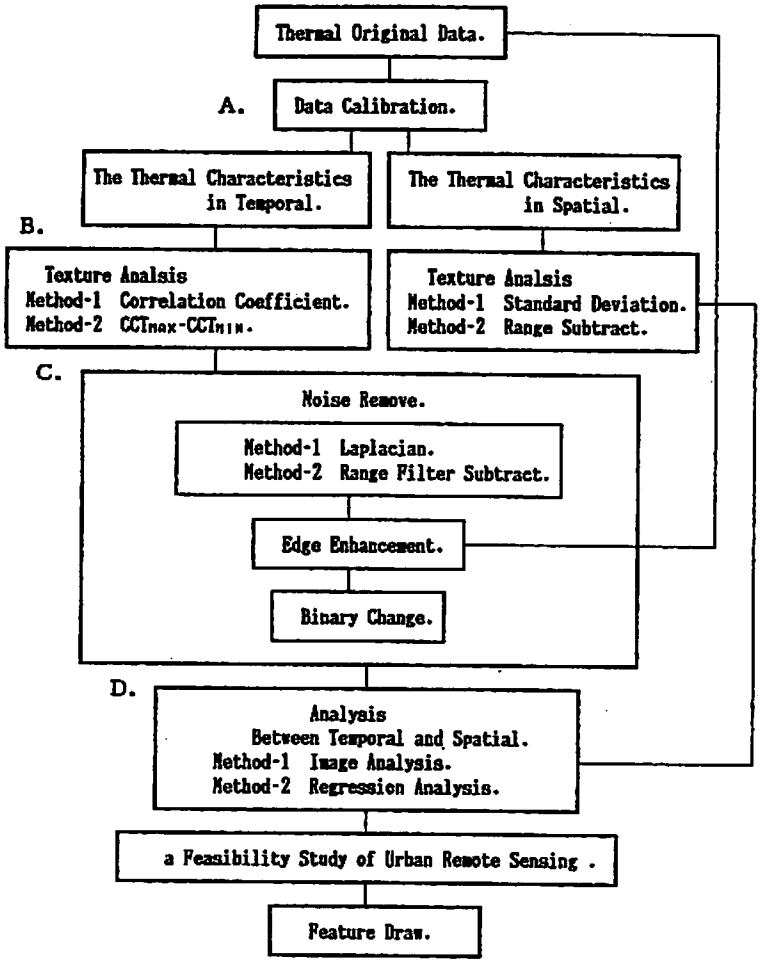

Fig. 1　FLOW of STUDY

3．Study Area and Data

This study has analyzed the data of Band－6/TM of LANDSAT－5. From the band 1,2,3,4 and 5 produced the analysis supported images which consist of colors-composite, vegetation and water area images.

The test site was selected the built-up area of TOKYO, where are densely populated and relatively devastated green area.

Remote sensing is an effective way to survey urban environmental analysis and authors have verified its usefulness, that means the application example mentioned here are now in developing stages but still by continuing the more renewable algolism, can be speeded up the process operations and gained the more better qualitative result.

Fig 2 and Fig 3 are the attribute of satellite images and the image 1,2,3,4 show the vegitation, water area, thermal and false color images.

BAND 1	0.45-0.52(30)
BAND 2	0.52-0.60(30)
BAND 3	0.63-0.69(30)
BAND 4	0.76-0.90(30)
BAND 5	1.55-1.75(30)
BAND 6	10.4-12.5(120)

Fig. 2 WAVELENGTH: μm
(Resolving Power:m)

PATH*ROW	107*35
EXPOSURE DATA	1.23.85 5.21.87 7.24.87 10.9,88
ORBIT	Sun-Synchronous Orbit
ALTITUDE	705km
ANGLE	98°
ORBITAL PRIOD	16Day
SENSOR	Thematic Mapper
VISIBLE/N.IR	4Band
IR	2Band
THERMAL. IR	1Band
RESOLVING POWER	30m (VISIBLE/N.IR/IR) 120m (THERMAL. IR)
SWATH WIDTH	185km

Fig. 3 LANDSAT/TM

Image. 1 VEGETATION IMAGE

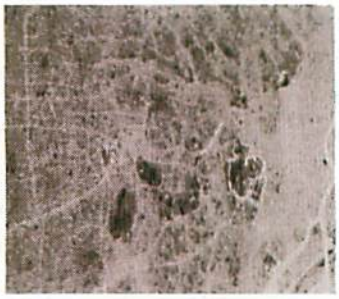

Image. 2 WATER IMAGE

Image. 3 THERMAL IMAGE

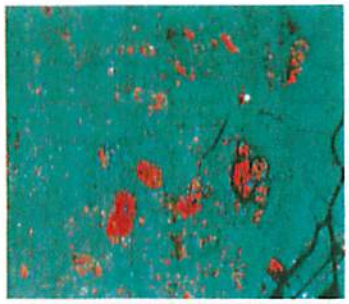

Image. 4 FALSE COLOR IMAGE

4. Image Parameter and Data Calibration

4. 1 Measurement of Image Parameters

Each image of thermatic mapper consists of 8 bits per one and describes as the digital number from 0 to 255, LANDSAT/TM has resolving power of 120m in thermal band and records the average radiance in 120m^2. This study covers the area of 400 x 512 pixels, that are equivalent to 204800 pixels.

Then, the radiance values are measured on the images and the radiance distribution is calculated for the extration of image parameters such as standard deviation, average, max. and min. values.

The difference of max. and min. values is called as dynamic range and also calculated from the radiance values mention above.

Dynamic range in thermal band of LANDSAT/TM is narrower than dynamic rang of other sensors, because of flight altitude of LANDSAT, that means, I.F.O.V.(Instantaneous Field of View) of the sonsors becomes more wider.

LANDSAT on low altitude needs to scan faster than other satellites, as the faster scanning doesn't give enough reflection and radiance energy.

Infrared radiance has the same problem of being narrow dynamic rang as other satellites. The image signal of infrared radiation records the strength radiance energy, then it doesn't need the sun source because the radiance energy of subject itself is measured.

That is the reason why band 6 is narrower than other band 1,2,3,4,5 and 7 in LANDSAT/TM and resolving power of band 6 is lower than other bands.

The Table 1,2,3 and 4 show the measured result of image parameters.

Table. 1　IMAGE PARAMETER on '85 23 JAN

	85' 23. JAN					
	CH1	CH2	CH3	CH4	CH5	CH6
CCTnum	204800	204800	204800	204800	204800	204800
CCTmin	20	15	15	5	5	75
CCTmax	100	60	85	70	155	10
CCTavg	71.46	27.90	29.85	22.57	29.70	89.69
CCTstd	71.56	28.66	29.99	22.90	30.76	89.76
CCTdyn	70	45	70	65	150	55

Table. 2　IMAGE PARAMETER on '87 21 MAY

	87' 21. MAY					
	CH1	CH2	CH3	CH4	CH5	CH6
CCTnum	204800	204800	204800	204800	204800	204800
CCTmin	85	25	20	10	0	120
CCTmax	255	165	205	220	255	175
CCTavg	125.76	49.22	51.50	57.26	72.51	151.51
CCTstd	124.25	49.57	52.18	58.78	74.00	48.14
CCTdyn	170	140	185	210	255	55

Table. 3　IMAGE PARAMETER on '87 24 JUL

	87' 24. JUL					
	CH1	CH2	CH3	CH4	CH5	CH6
CCTnum	204800	204800	204800	204800	204800	204800
CCTmin	70	20	15	5	0	135
CCTmax	255	185	215	180	255	180
CCTavg	117.29	47.42	48.95	52.93	66.88	152.30
CCTstd	118.21	48.65	50.60	54.46	68.56	47.57
CCTdyn	185	165	200	175	255	25

Table. 4　IMAGE PARAMETER on '87 9 OCT

	87' 9. OCT					
	CH1	CH2	CH3	CH4	CH5	CH6
CCTnum	204800	204800	204800	204800	204800	204800
CCTmin	55	15	10	0	0	125
CCTmax	225	130	180	140	280	155
CCTavg	76.45	30.70	32.48	30.85	42.23	141.76
CCTstd	76.82	31.04	33.11	31.79	43.58	141.89
CCTdyn	170	115	170	140	250	30

4.2 Data Calibration using Normalized Equation

As mentioned above, images have the dynamic rangs which are changeable in certain limit. When multi - temporal images compare and analyze, the operation of image scaling is performed so as to being the same level in image process.

(1) Concept of Image Scaling

On the image is measured the range width with being the difference of max. and min. CCT count which is called as dynamic range.

The dynamic rang of multi－temporal images show the seasonal difference and the level of thermal distribution. The dynamic range of one single season is unified within the seasonal band. Here shows one example, there are two images, IMG 1 (u, v) and IMG 2 (u, v) with DYN 1 is united in IMG 2 (u,v) with DYN 2.

The selecting conditons for IMG 1 (u,v) are as follows:

Condition 1
Being CCT dyn with IMG 1 > CCT dyn with IMG 2

Condition 2
Being CCT std with IMG 1 > CCT std with IMG 2
CCT std is standard deviation in images.

Conditon 3
Histogram of images presupposes is Gaussian distribution.

Condition 4
Correlation coefficient between thermal image
and ground truth data is high.

In the first place, original image is done regression analysis as explaining variable the IMG 2 and as unexplaining varible the IMG 1.

Then, normal equation(1) of the regression and correlation coefficient is as follows:

$$IMG1 = IMG2 \cdot a + b \qquad (1)$$

correlation coefficient r

The a in equation (1) is called as the inclined scaling factor and b independent factor that means distance from the origin to the axis .

A new image ＩＭＧ２' is acquired by putting equation (2) into ＩＭＧ２.

$$IMG2' = IMG2 \cdot a + b \qquad (2)$$

This ＩＭＧ２' is called as the scaling image. In order to verify the ＩＭＧ２' , correlation between ＩＭＧ１ and IMG2' is calculated using equation(3).

$$IMG1 = IMG2' \cdot a' + b' \qquad (3)$$

correlation coefficient r'

If this result is satisfied with the following verification items, this scaling is judged to be effective.

The verification condition:

Condition 1
Being r'>r

r':correlation coefficient of ＩＭＧ１ and ＩＭＧ２'
r :correlation coefficient of ＩＭＧ１ and ＩＭＧ２

Condition 2
a' is closer to 1 than a.

a':inclination in normal equation of ＩＭＧ１ and ＩＭＧ２'
a :inclination in normal equation of ＩＭＧ１ and ＩＭＧ２

Condition 3
Histogram of ＩＭＧ２' is more similar to Gaussian distribution than Histogram of ＩＭＧ１.

(2) Selection of calibration image

The data on July 24, 1987 were used for this study, the reason is clear as mentioned before.

At first the analysis is performed using the main images, the regression analysis are performed between this main image and other three images, which given the calibration parameter with other three images that are calibrated.

Table 5 shows the result and Fig. 4 to 6 are the correlation figure.

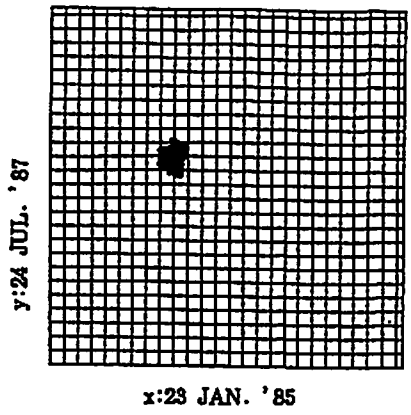

Fig. 4 CORRELATION FIGURE

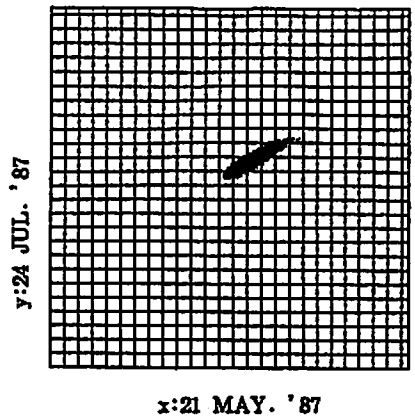

Fig. 5 CORRELATION FIGURE

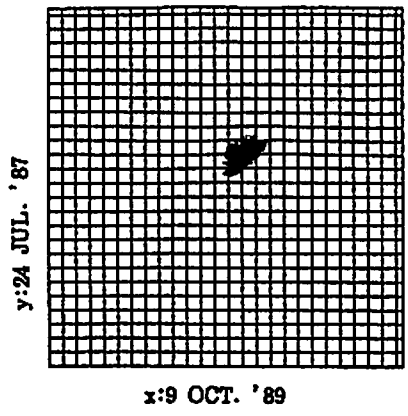

Fig. 6 CORRELATION FIGURE

Table. 5 REGRESSION FORMULA and CORRELATION COEFFICIENT before CALIBRATION

Y: 87' 24. JUL

	REGRESSION FORMULA	CORRELATION CIEPPICIENT
X: 85' 23. JAN	Y= -0.149X+165.881	-0.086
X: 87' 21. MAY	Y= 0.566X+66.632	0.932
X: 86' 9. OCT	Y= 0.654X+59.611	0.752

The calculated inclined and independent factors are multiplied and added to the original images. There are shown from equation (4) to (6).

$$CCT1' = -0.149 * CCT1 + 165.881 \quad (4)$$
$$CCT5' = 0.566 * CCT5 + 66.632 \quad (5)$$
$$CCT10' = 0.654 * CCT10 + 59.611 \quad (6)$$

CCT1' : image on January 23 after the calibration
CCT1 : original data on January 23
CCT5' : image on May 21 after calibration
CCT5 : original data on May 21
CCT10' : image on October 9 after calibration
CCT10 : original data on October 9

Table 6 shows the result for verification, of the images such as CCT1', CCT5' and CCT10'.

Table. 6 REGRESSION FORMULA and CORRELATION COEFFICIENT after CALIBRATION

Y: 87' 24. JUL

	REGRESSION FORMULA	CORRELATION COEFFICIENT
X: 85' 23. JAN	Y= -0.090X+166.561	-0.089
X: 87' 21. MAY	Y= 0.985X+22.947	0.950
X: 86' 9. OCT	Y= 0.988X+0.569	0.820

5. Extraction of informations using texture analysis

Texture consist of 4 types which each define 5 x 5 size, 2 types are temporal informations, but other 2 are spatial informations.

5.1 Extraction of temporal informations

1) Method of Correlation Coefficient

Texture of correlation is imaged the correlation coefficient in partial spatial filter on temporal thermal images. The Fig 7 shows the flow chart. Equation (7) described the processing formula and Image 5 is the result of calcutaion.

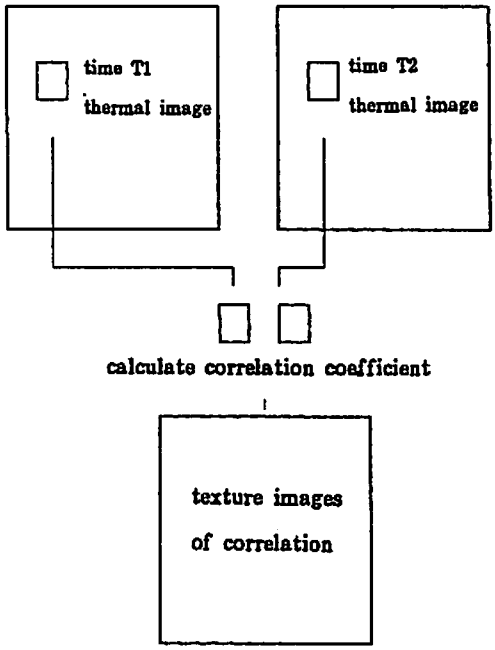

Fig. 7 TEXTURE IMAGE of CORRELATION COEFFICIENT

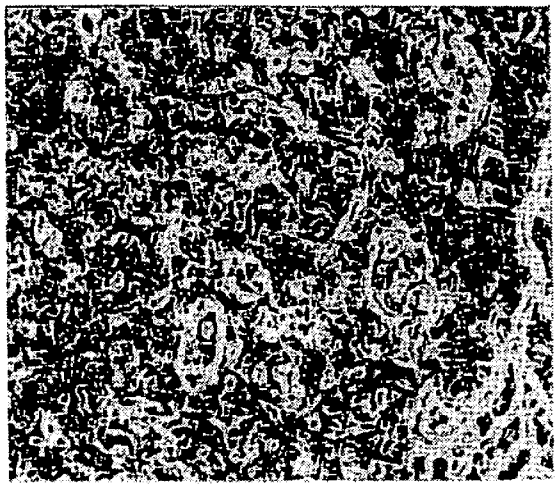

Image. 5 TEXTURE of CORRELATION COEFFICIENT

$$cor(u,v)=\frac{\sum_{j=v+2}^{v-2}\sum_{j=v+2}^{v-2}\{(Xij-Xavg(u,v))\ (Yij-Yavg(u,v))\}}{\sqrt{\{\sum_{j=v+2}^{v-2}\sum_{j=v+2}^{v-2}\{(Xij-Xavg(u,v))^2\}\}}\sqrt{\{\sum_{j=v+2}^{v-2}\sum_{j=v+2}^{v-2}\{(Yij-Yavg(u,v))^2\}\}}}$$

$$IMGcor=cor(u,v)\cdot G+OF \quad (7)$$

Xij: CCT count of time T 1 period in filter

Xavg(u,v): average CCT count of T1 period in filter

Yij: CCT count of time T 2 period in filter

Yavg(u,v): average CCT count of time T 2 period in filter

cor(u,v): correlation coefficient in filter

G: gain factor

OF: offset factor

IMGcor: texture image of correlation coefficient

2) method of Max.−Min.

The texture of max.−min. is imaged the result of subtraction works−to subtract min. CCT from max. CCT in filter−, next the texture image is imaged the result of subtracting certain time images from subtraction of another time image.

Fig 8. shows the flow chart, computed formula shows in equation(8), result of calculation shows in image 6.

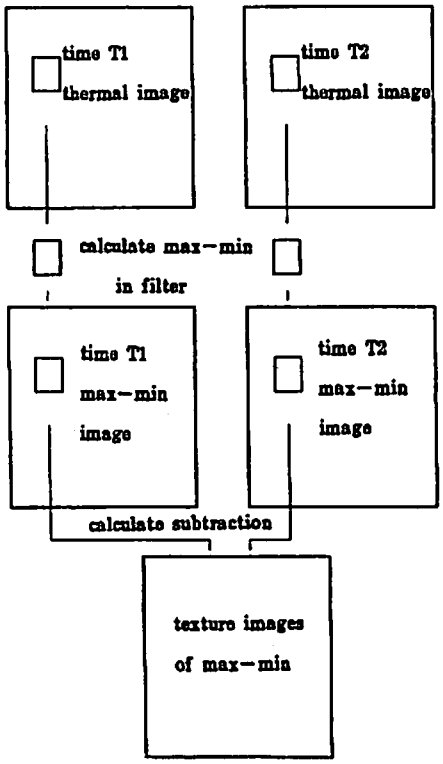

Fig. 8　TEXTURE IMAGE of MAX.−MIN.

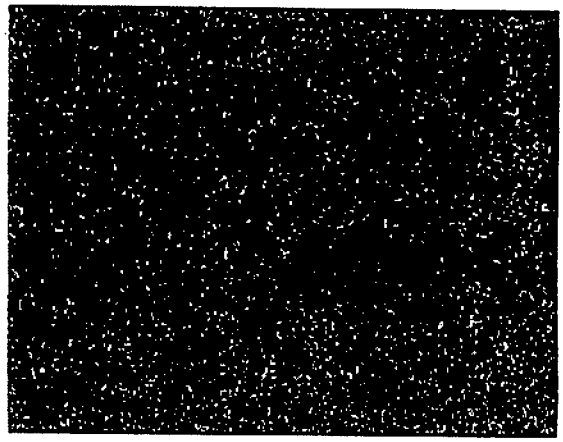

Image. 6　TEXTURE of MAX.−MIN.

$$Xmax(u,v)=max(X1, X2, \cdots\cdots X25)$$
$$Xmin(u,v)=min(X1, X2, \cdots\cdots X25)$$

$$Ymax(u,v)=max(Y1, Y2, \cdots\cdots Y25)$$
$$Ymin(u,v)=min(Y1, Y2, \cdots\cdots Y25)$$

$$dTT1=Xmax(u,v)-Xmin(u,v),\quad dTT2=Ymax(u,v)-Ymin(u,v)$$

$$IMGrag=ABS\ (dTT1-dTT2)\ \cdot G-OF \qquad (8)$$

Xmax(u,v) : max CCT count of time T 1 period in filter

Xmin(u,v)：min CCT count of time T 1 period in filter

Ymax(u,v)：max CCT count of time T 2 period in filter

Ymin(u,v)：min CCT count of time T 2 period in filter

dTT1： substraction of time T 1 period between max CCT and min CCT in filter

dTT2： substraction of time T 2 period between max CCT and min CCT in filter

G：gain factor

OF：offset factor

IMGrag：texture image of max - mix

5.2 Extraction of Spatial Information

1)Method of Standard Deviation

Texture of standard deviation is imaged standard deviation in spatial filter of thermal image of one period.

Fig 9 shows the flow chart, computed formula shows equation (9) and result of calcultaion shows in image 7.

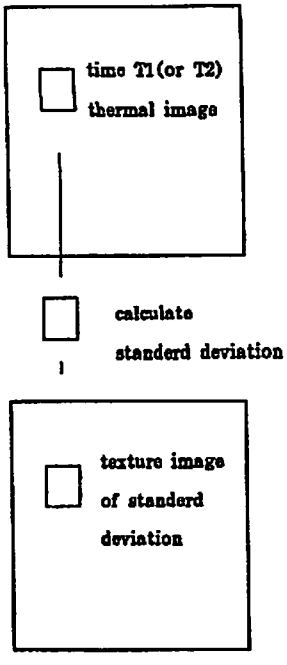

Fig. 9 TEXTURE IMAGE of STANDARD DEVIATION

Image. 7 TEXTURE of STANDARD DEVIATION

$$Xstd = \sqrt{\{\sum_{j=v+2}^{v-2} \sum_{j=v+2}^{v-2} \{ (Xij - Xavg(u,v))^{2} \}}$$

$$IMGstd = Xstd \cdot G + OF \qquad (9)$$

Xij : CCT count of time T 1 period in filter

Xavg(u,v) : average CCT count of time T 1 period in filter

G : gain factor

OF : offset factor

IMGstd : texture image of standerd deviation

2) Method of Range Subtraction

Texture of range subtraction is imaged as subtraction of max CCT and min CCT in same period images.

Fig 10. shows the flow chart, computed formula shows in quation (10), result of calculation shows in image 8.

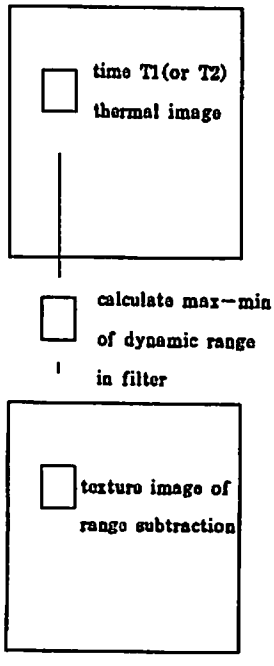

Fig. 10 TEXTURE IMAGE of RANGE SUBTRACTION

Image. 8 TEXTURE of RANGE SUBTRACTION

$$dTT1 = Xmax(u,v) - Xmin(u,v)$$

$$IMGsub = dTT1 \cdot G + OF \quad (10)$$

Xmax(u,v)：max CCT of one period in filter
Xmin(u,v)：min CCT of one period in filter
dTT1：dynamic range
G：gain factor
OF：offset factor
IMGsub：texture image of Range subtraction

6. Noise remove

6.1 Necessity of noise Remove

Texture images bring noise generation when texture is computed by spatial filtering method.

Filter used in texture analysis enhances quantity of texture when it passes different land covers.

Enhanced texture, it's places where consist of a variety land core, i. e, differential land cover areas shows a thermal fault. This phenomena appear remarkably on texture images which are based upon the correlation coefficient. Because the places where dynamic range is wide, show high value in correlation coefficient, but the places where dynamic range is narrow, show low value.

The Fig 11 and 12 show concept mentioned above. Fig 11 shows the distribution of uniform land cover, but Fig 12 for being not uniform.

The correlation coefficient shows high by placing a filter on the land cover being not uniform. The noise are removed by edge enhanced thermal images.

Full color edge enhanced images are transformed into binary image data. The threshold is determinated by distinctive method of histogram.

In the end, noise of texture images of correlation coefficient are removed by binary edge enhanced images.

In this study, two methods are presented with LAPLACIAN－FILTER and RANG－FILTER and finally The RANG－FILTER is suggested in this study.

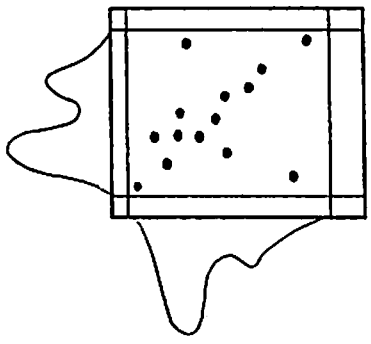

Fig. 11 WIDE DYNAMIC RANGE

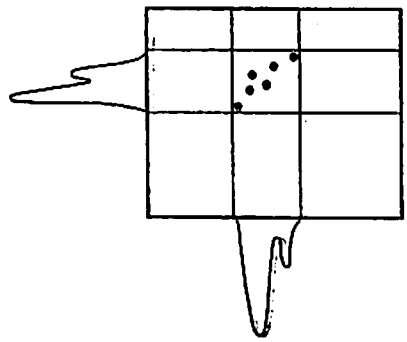

Fig. 12 NARROW DYNAMIC RANGE

6.2 Noise Remove by LAPLACIAN-FILTER

The LAPLACIAN - FILTER is one of industrial image processing for image enhancement. The enhanced image process is called as image differential operation too and is used mainly for extracting the characteristic feature in image processing using pattern recognition. This method is performed by laplacian filtering for the area defined 8 pixel including its surrounding.

Laplacian filter show as Fig 13. The enhanced images of full color edge show in equation (11) and equation (12) with binary edge.

$$\begin{bmatrix} 1 & 1 & 1 \\ 1 & -8 & 1 \\ 1 & 1 & 1 \end{bmatrix}$$

Fig. 13 LAPLACIAN FILTER

$$IMG^{lp}_{Egde} = \nabla^2 IMG_{org} \quad (11)$$

$$IMG^{lp}_{cor} = IMG_{cor} - IMG^{lp}_{Egde} \quad (12)$$

IMG^{lp}_{Egde}: Full color edge enhanced image removed by laplacian

∇^2 :laplacian

IMG_{org} :thermal original image

IMG_{org} :texture image of coefficient

IMG^{lp}_{org} : Images removed noise from texture of correlation coefficient

6.3 Noise Remove by RANGE-FILTER

Normally the Laplacian filter is popularly used for process the edge enhancemant, but not always suitable for the industrial image processing.

Then, this study has surveied about availability of edge remove with RANGE－FILTER. The LAPLACIAN－FILTER has the adaptability for anything except thermal fault.

Therefore, if informations inside filter are clear for the edge enhancement, Laplacian Filter can be used with flexibility.

However, RANGE－FILTER tends strongly to enhance edges. The area of enhanced edge in the image are larger.

Then, the method of LAPLACIAN - FILTER and RANG－FILTER have good and bad points as noise remove method.

This study reported on RANGE－FILTER method because this study aims at examining texture algorism too.

The edge of RANGE－FILTER defines as equation (13) and equation (14) shows the processing formula of noise remove.

$$X_{max}(u,v) = max(X1,\ X2,\ \cdots\cdots X25)$$

$$X_{min}(u,v) = min(X1,\ X2,\ \cdots\cdots X25)$$

$$IMG^{rng}_{Edge} = (X_{max}(u,v) - X_{min}(u,v)) * G + OF \quad (13)$$

$$IMG^{rng}_{cor} = IMG^{rng}_{cor} - IMG^{rng}_{Edge} \quad (14)$$

$X_{max}(u,v)$: max CCT count value in partial filter

$X_{min}(u,v)$: min CCT count value in partial filter

IMG^{rng}_{Edge} : edge enhanced images by RANGE - FILTER

IMG^{rng}_{cor} : noise removed image from temporal thermal texture images using correlation coefficient

G ：gain factor

ＯＦ：offset factor

7．Integrated Analysis of Multi-temporal and Spatial Informations

7.1 Image Analysis

As mentioned above, multi-temporal informations are extracted by two algorism and spatial informations are extracted by two another algorism too.

The noise remove were performed on texture images using correlation coefficient.

The texture of multi-temporal and spatial are calculated by two algorisms, each extracted informations were different.

As the first priority, the analysis of temporal and spatial thermal texture were performed.

When texture images compare and analyze the image analysis in this study intends to interpret from the images the differences between texture of multi-temporal and spatial.

Subtractive equation shows as equation(15) which calcurates absolute subtraction. This equation means that if CCT count value of ＩＭＧ sub converges to near zero, then the values surrounding zero's area are difficult to be change for the thermal texture that means the higher the CCT count values is, the more changeable.

Subtractive images are shown on from image 9 to image 11 in which the characteristics of image can be seen clearly.

Image. 9 SUBTRACTIVE IMAGE

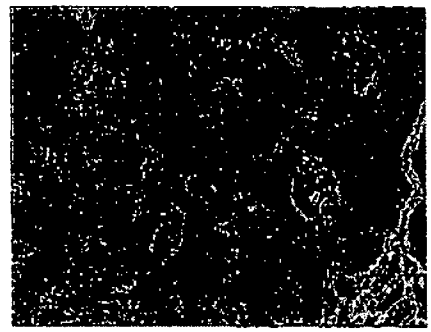

Image.10 SUBTRACTIVE IMAGE

Image.11　SUBTRACTIVE IMAGE

$$IMG_{sub} = ABS\ (IMGT - IMGS) \quad (15)$$

IMGsub：Subtractive image
IMGT：Multi－temporal image
IMGS：Spatial information image

7.2 Regression Analysis

To verify the regression analysis, image was analyzed using equation (16) and correlation coefficient was calculated.

Table 7 to Table 12 show correlation coefficient, texture images of correlation coefficient were used as the inducing variable and texture images of standard deviation and range subtraction were used as the object variable.

Table 13 to Table 18 show correlation coefficient, texture image of max.－min. were used as the inducing variable and texture image of standerd deviation and range subtraction were used as the object variable.

Table 7 CORRELATION between MULTI−TEMPORAL and SPATIAL

MULTI−TEMPORAL AND SPATIAL			CORRELATION
1/23 5/21 (CORRELATION COEFFICIENT)	AND	1/23 (STANDERD DEVIATION)	0.658
1/23 5/21 (CORRELATION COEFFICIENT)	AND	5/21 (STANDERD DEVIATION)	0.651
1/23 5/21 (CORRELATION COEFFICIENT)	AND	1/23 (RANGE SUBTRACTION)	0.681
1/23 5/21 (CORRELATION COEFFICIENT)	AND	5/21 (RANGE SUBTRACTION)	0.541

Table 8 CORRELATION between MULTI−TEMPORAL and SPATIAL

MULTI−TEMPORAL AND SPATIAL			CORRELATION
1/23 7/24 (CORRELATION COEFFICIENT)	AND	1/23 (STANDERD DEVIATION)	0.695
1/23 7/24 (CORRELATION COEFFICIENT)	AND	7/24 (STANDERD DEVIATION)	0.751
1/23 7/24 (CORRELATION COEFFICIENT)	AND	1/23 (RANGE SUBTRACTION)	0.585
1/23 7/24 (CORRELATION COEFFICIENT)	AND	7/24 (RANGE SUBTRACTION)	0.659

Table 9 CORRELATION between MULTI−TEMPORAL and SPATIAL

MULTI−TEMPORAL AND SPATIAL			CORRELATION
1/23 10/9 (CORRELATION COEFFICIENT)	AND	1/23 (STANDERD DEVIATION)	0.891
1/23 10/9 (CORRELATION COEFFICIENT)	AND	10/9 (STANDERD DEVIATION)	0.955
1/23 10/9 (CORRELATION COEFFICIENT)	AND	1/23 (RANGE SUBTRACTION)	0.810
1/23 10/9 (CORRELATION COEFFICIENT)	AND	10/9 (RANGE SUBTRACTION)	0.944

Table 10 CORRELATION between MULTI−TEMPORAL and SPATIAL

MULTI−TEMPORAL AND SPATIAL			CORRELATION
5/21 7/24 (CORRELATION COEFFICIENT)	AND	5/21 (STANDERD DEVIATION)	0.929
5/21 7/24 (CORRELATION COEFFICIENT)	AND	7/24 (STANDERD DEVIATION)	0.899
5/21 7/24 (CORRELATION COEFFICIENT)	AND	5/21 (RANGE SUBTRACTION)	0.805
5/21 7/24 (CORRELATION COEFFICIENT)	AND	7/24 (RANGE SUBTRACTION)	0.808

Table 11 CORRELATION between MULTI−TEMPORAL and SPATIAL

MULTI−TEMPORAL AND SPATIAL			CORRELATION
5/21 10/9 (CORRELATION COEFFICIENT)	AND	5/21 (STANDERD DEVIATION)	0.559
5/21 10/9 (CORRELATION COEFFICIENT)	AND	10/9 (STANDERD DEVIATION)	0.485
5/21 10/9 (CORRELATION COEFFICIENT)	AND	5/21 (RANGE SUBTRACTION)	0.501
5/21 10/9 (CORRELATION COEFFICIENT)	AND	10/9 (RANGE SUBTRACTION)	0.455

Table 12 CORRELATION between MULTI−TEMPORAL and SPATIAL

MULTI−TEMPORAL AND SPATIAL			CORRELATION
7/24 10/9 (CORRELATION COEFFICIENT)	AND	7/24 (STANDERD DEVIATION)	0.699
7/24 10/9 (CORRELATION COEFFICIENT)	AND	10/9 (STANDERD DEVIATION)	0.590
7/24 10/9 (CORRELATION COEFFICIENT)	AND	7/24 (RANGE SUBTRACTION)	0.587
7/24 10/9 (CORRELATION COEFFICIENT)	AND	10/9 (RANGE SUBTRACTION)	0.477

Table.13 CORRELATION between MULTI−TEMPORAL and SPATIAL

MULTI−TEMPORAL AND SPATIAL	CORRELATION
1/23 5/21 (MAX - MIN) AND 1/23 (STANDERD DEVIATION)	0.488
1/23 5/21 (MAX - MIN) AND 5/21 (STANDERD DEVIATION)	0.319
1/23 5/21 (MAX - MIN) AND 1/23 (RANGE SUBTRACTION)	0.329
1/23 5/21 (MAX - MIN) AND 5/21 (RANGE SUBTRACTION)	0.301

Table.14 CORRELATION between MULTI−TEMPORAL and SPATIAL

MULTI−TEMPORAL AND SPATIAL	CORRELATION
1/23 7/24 (MAX - MIN) AND 1/23 (STANDERD DEVIATION)	0.328
1/23 7/24 (MAX - MIN) AND 7/24 (STANDERD DEVIATION)	0.299
1/23 7/24 (MAX - MIN) AND 1/23 (RANGE SUBTRACTION)	0.337
1/23 7/24 (MAX - MIN) AND 7/24 (RANGE SUBTRACTION)	0.221

Table.15 CORRELATION between MULTI−TEMPORAL and SPATIAL

MULTI−TEMPORAL AND SPATIAL	CORRELATION
1/23 10/9 (MAX - MIN) AND 1/23 (STANDERD DEVIATION)	0.582
1/23 10/9 (MAX - MIN) AND 10/9 (STANDERD DEVIATION)	0.571
1/23 10/9 (MAX - MIN) AND 1/23 (RANGE SUBTRACTION)	0.521
1/23 10/9 (MAX - MIN) AND 10/9 (RANGE SUBTRACTION)	0.549

Table.16 CORRELATION between MULTI−TEMPORAL and SPATIAL

MULTI−TEMPORAL AND SPATIAL	CORRELATION
5/21 7/24 (MAX - MIN) AND 5/21 (STANDERD DEVIATION)	0.642
5/21 7/24 (MAX - MIN) AND 7/24 (STANDERD DEVIATION)	0.599
5/21 7/24 (MAX - MIN) AND 5/21 (RANGE SUBTRACTION)	0.628
5/21 7/24 (MAX - MIN) AND 7/24 (RANGE SUBTRACTION)	0.511

Table.17 CORRELATION between MULTI−TEMPORAL and SPATIAL

MULTI−TEMPORAL AND SPATIAL	CORRELATION
5/21 10/9 (MAX - MIN) AND 5/21 (STANDERD DEVIATION)	0.481
5/21 10/9 (MAX - MIN) AND 10/9 (STANDERD DEVIATION)	0.329
5/21 10/9 (MAX - MIN) AND 5/21 (RANGE SUBTRACTION)	0.399
5/21 10/9 (MAX - MIN) AND 10/9 (RANGE SUBTRACTION)	0.209

Table.18 CORRELATION between MULTI−TEMPORAL and SPATIAL

MULTI−TEMPORAL AND SPATIAL	CORRELATION
7/24 10/9 (MAX - MIN) AND 7/24 (STANDERD DEVIATION)	0.322
7/24 10/9 (MAX - MIN) AND 10/9 (STANDERD DEVIATION)	0.197
7/24 10/9 (MAX - MIN) AND 7/24 (RANGE SUBTRACTION)	0.274
7/24 10/9 (MAX - MIN) AND 10/9 (RANGE SUBTRACTION)	0.090

$$cor = \frac{\sum_{j=1}^{400}\sum_{i=1}^{512}\{ (Xij - Xavg(u,v))\ (Yij - Yavg(u,v)) \}}{\sqrt{\{\sum_{j=1}^{400}\sum_{i=1}^{512}\{ (Xij - Xavg(u,v))^2\}}\sqrt{\{\sum_{j=1}^{400}\sum_{i=1}^{512}\{ (Yij - Yavg(u,v))^2\}}} \quad (16)$$

Xij: multi - temporal image of thermal texture

Xavg(u,v): average CCT count value

of multi - temporal image of thermal texture

Y ij: spatial image

Y avg(u,v): average CCT count value
of multi－temporal image of termal texture

cor: correlation coefficient

8. Result of Analysis

8.1 Image Calibration

As the result of calibration using normal equation of correlation coefficient, the dynamic range is unified.

So far calibration method using regression formula has not been tried for LANDSAT / TM data at all. Because dynamic range of LANDSAT/TM is narrow, that means, it causes the difficult problem for thermal image processing. The original images of data have been normalyzed and have been used only normalyzed parameters measured only histogram, but in fact, these parameters must use not only histogram but also satellite parameter.

These things cause that end users do not know informations of all satellite system, geometric, systematic corrections etc, so result of each study is not adjustable and dependent.

Though satellite and sensor parameters are unknown, in order to examine texture algorism and characteristics of thermal multi - temporal and spatial texture, it is fully satisfied to do the calibrations with histogram parameters.

8.2 Thermal Environmental Conditons from Multi-temporal and Spatial Informations

Multi - temporal thermal informations were extracted by texture images of correlation coefficient and max. - min. methodology and spatial informations were extracted by texture images of standerd deviation and range subtraction.

Both were compared by images processing and regression analysis. Image processing was estimated by high and low of CCT count values, calculated from the absolute subtraction, that means, the places where CCT count value is law, are having the same thermal behave. Regression analysis was estimated by correlation coefficient.

As a result, in method of image analysis, texture image of correlation coefficient as multi－temporal image can extract difference between multi－temporal and spatial informations, and in method of regression analysis, texture image of max.－min. as multi－temporal extract difference

between multi－temporal and spatial information, if method of image analysis use texture image of max.－min., images are hard to look due to random pattern, so image information do not acquire and if method of regression analysis use texture image of correlation coefficient, correlation ceofficient is very bad.

Method of image processing make out that black part in image (low CCT) shows that same behavior between multi－temporal and spatial.

White area (high CCT) to block area are different behavior－, rever, vegetation, sea coast－, different behaved area is that either multi－temporal or spatial characteristics is higher. These things do not find because of absolute subtraction.

Then method of regression analysis verify image processing using coefficient, this method analyze except rever, vegetation, sea coast where these area are different behavior.

Specially, it is very high to correlation coefficient between multi - temporal image (by texture image of correlation coefficient) in FEB.23 and OCT.9 and spatial image (by texture image of standerd deviation) in OCT.9, thermal characteristics of both is same behavior.

The result of study could acquire high potentiality to estimate urban thermal environmental information from in spatial to multi－temporal.

References

1)Gene A. Thorley et al.
Manual of Remote Sensing
American Society of Photogrammety,1983

2)Ohkubo•Nagata
Urban Climatology
Asakura publishing Co.Ltd.,1974

3)Toshio Ojima
Remote Sensing Series:Cities
Asakura publishing Co. Ltd.,1980

4)Remote Sensing Technology Center of JAPAN
Handbook on Data Handling of The Earth Observation
Remote Sensing Techonology Center of Japan,1990

5)Syunji Murai et al.
Remote Sensing Note
Japan Association of Remote Sensing

Gihodo publishing Co. Ltd.,1975

6)Uchida,Rikimal,Oshima

Extracted Ground thermal characteristics

using LANDSAT/TM Data

The Japan Society of Civil Engineers

Annual Meeting of Kanto-District.

Proceedings : pp.242-243,1990

7)Uchida,Rikimal,Oshima

Extracted Thermal Environmental

using Thermal Texture

The Japan Society of Photogrammetry and Remote Sensing

Annual Meeting 1990

8)Tetsurou Uchida

Texture Analysis of Thermal Characteristics

using Spatial Filter

Bulletin of Graduate Studies in Hosei University

No.26 pp.293-296,1991

9)Oshima,Ucida

Study of Urban Thermal Environmental

The Japan Society of Civil Engineers

Annual Meeting of Kanto District.

Proceedings : pp.214-215,1991

10)Tshipolot,Kojima,Oobayashi

On the Effective Sparial Information for

the Multispectral Classification

Journal of Japan Society of Remote Sensing

No.11-3 pp 21-33 1991